論文 / 著書情報
Article / Book Information

Title	Characteristics of a Full-scale Multi-layered Viscoelastic Damper under Long-duration Loading
Authors	Dave M.Osabel, Daiki Sato, Kazuhiko Kasai
Citation	Proceedings of the 12th Pacific Structural Steel Conference, , ,
Pub. date	2019, 11

CHARACTERISTICS OF A FULL-SCALE MULTI-LAYERED VISCOELASTIC DAMPER UNDER LONG-DURATION LOADING

Dave M. Osabel*, Daiki Sato and Kazuhiko Kasai****

* Architecture and Building Engineering Department, Tokyo Institute of Technology, Japan
e-mail: osabel.d.aa@m.titech.ac.jp

** Future Interdisciplinary Research of Science and Technology (FIRST), Tokyo Institute of Technology, Japan
e-mails: sato.d.aa@m.titech.ac.jp, kasai.k.ac@m.titech.ac.jp

Keywords: multi-layered viscoelastic damper, long-duration loading, heat generation, 3D heat transfer analysis, 3D finite element model.

Abstract. *Studies showed that properly employed viscoelastic (VE) dampers can mitigate wind-induced vibrations of tall buildings. These devices work by absorbing kinetic energy and converting it to small amount of heat. Since VE dampers are temperature- and frequency-sensitive, increase of temperature results to decrease of VE damping properties. In their past studies on simple lap-type two layered VE dampers under long-duration loading, the authors experimentally and analytically showed the effects of heat generation and heat transfer. Heat was effectively dispersed to the surrounding air bringing the simple VE damper to thermal equilibrium. Nowadays, VE dampers are made of several thin layers of VE materials, and due to high computational cost in carrying-out finite element analysis, few analytical studies are done for full-scale multi-layered VE dampers. This paper addresses this matter by implementing the previously proposed three-dimensional model of the co-authors into a multi-layered VE damper under long-duration sinusoidal loading, and results are verified with experiment. It shows that the 3D-FEM technique can be used to predict the temperature-dependency of a multi-layered VE damper.*

1 INTRODUCTION

1.1 Viscoelastic dampers and their early building applications

As the name implies, viscoelastic (VE) materials act partly as viscous material that can absorb or dissipate energy, and partly as an elastic material that can resist deformation. One practical use of VE material is in the field of structural engineering, i.e., VE dampers to dampen structural vibrations. Figure 1a is an example of the earliest form of VE dampers [1] installed in buildings to control vibrations induced by earthquake and/or strong wind. These early devices are made by sandwiching two small layers of VE materials between steel plates. Through the shear deformation of the steel-laminated VE materials, kinetic energy is absorbed and converted to a small amount of heat within the VE material [2].

The World Trade Center in New York, USA (built 1973) and Columbia Seafirst Center in Seattle, USA (built 1982) are among the first buildings installed with VE dampers which effectively reduced their wind-induced sway [3, 4]. Figure 1b shows how the small-scale VE dampers were installed in the 10^{th} to 110^{th} floors of the World Trade Center [1]. Despite the small form factor of these early VE dampers, they collectively suppress the structural vibration.

1.2 Full-scale multi-layered viscoelastic dampers

With the advancement of the manufacturing technology, it is now relatively easy to make VE dampers with several steel-sandwiched VE materials. Among the past experimental studies on multi-layered VE dampers are those of: Sato *et al*. [5] on an 8-layer and a 10-layer brace-type VE dampers, and Montgomery and Christopoulus [6] on a 15-layer and 17-layer viscoelastic coupling dampers (replacing outrigger beams). Both of these works considered relatively long-duration loadings to capture the aspects of heat generation and heat transfer in the behavior of VE dampers as it is known that VE materials have temperature and frequency dependencies.

1.3 Objectives and scopes

Most of the experimental investigations done in the past were at a fairly warm ambient temperature, ranging from 20°C to 30°C. In temperate countries such as Japan, VE dampers installed in buildings can be subjected to extreme low (0°C) and high (40°C) temperatures. Since the initial temperature of the VE damper (prior to any excitations) is highly dependent on

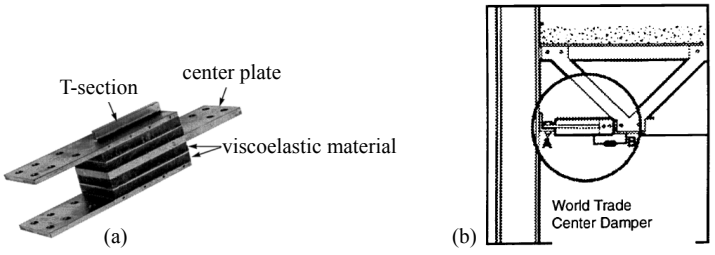

Figure 1. (a) Earliest form of viscoelastic damper, and (b) installation in the World Trade Center [1].

surrounding air temperature, it is imperative to investigate VE dampers under extreme low or high ambient temperatures. The authors addressed this by conducting a long-duration loading test on a full-scale VE damper under a low ambient temperature.

The authors also carried out an analytical investigation of the full-scale VE damper specimen. They adopted the previously proposed model of Kasai *et al*. [7] which combines static analysis and heat transfer analysis using three-dimensional finite element method.

2 LONG-DURATION HARMONIC LOADING TEST

2.1 Test setup

Figure 2a shows the full-scale VE damper used in the experiment. The experiment was conducted in one of the testing laboratories of Tokyo Institute of Technology (Suzukakedai Campus), Japan. It does not have any temperature control mechanism so the outdoor temperature is the primary factor affecting the indoor ambient temperature. As it was desired to investigate the VE damper's behavior under low ambient temperature, the experiment was done during the winter season in Japan. To avoid irregular fluctuation of indoor ambient temperature caused by outdoor wind, all wide-access doors were closed.

Figure 2b shows the schematic diagram of the experiment. The VE damper was placed horizontally on the test rig with its left end attached to a fix support while its right end attached to a slider support. Deformations were introduced to the assembly by the dynamic actuator. An amplification mechanism was provided between the dynamic actuator and the slider. Ideally by geometry, the amplification was in a factor of 2.0, i.e., slider deformation u_{slider} = 2 times the actuator deformation u_{act}. However, this cannot be true for all situations, thus, strain gage type transducers were installed at key locations to measure the actual deformations. Note that the damper deformation u_d refers to the deformation of the VE laminations.

2.2 Damper specimen

The full-scale damper tested had 6 layers of ISD111 type VE material and each had a thickness of 8 mm. Figure 2c shows the dimensions of the VE laminations. The total shear area A_s = 8,544 cm^2. The VE material property provided by the

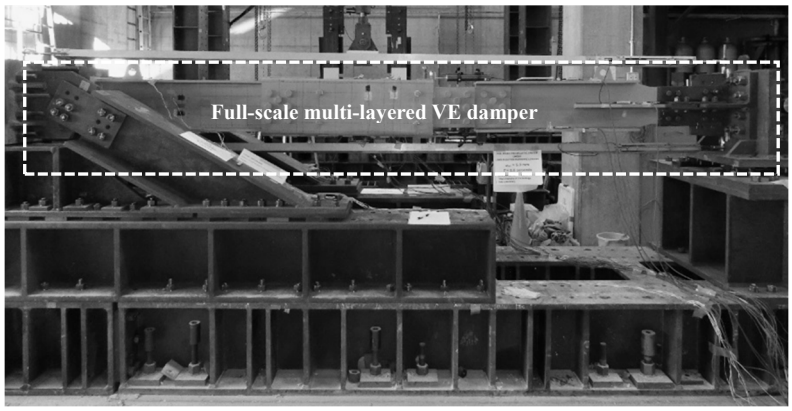

(a) VE damper test specimen.

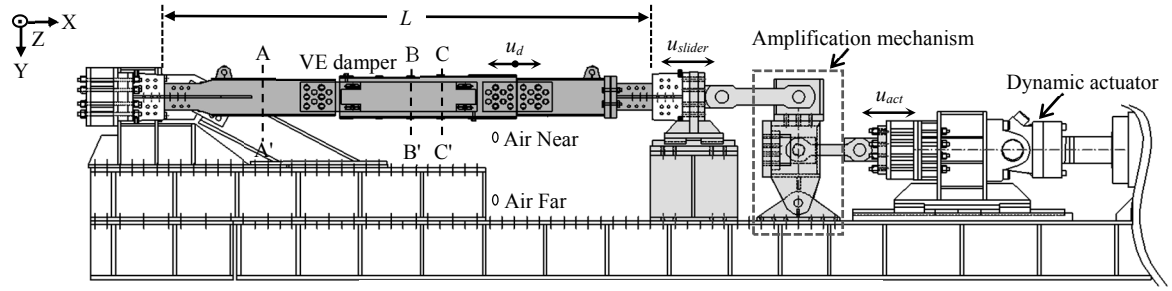

(b) Schematic diagram of the test setup.

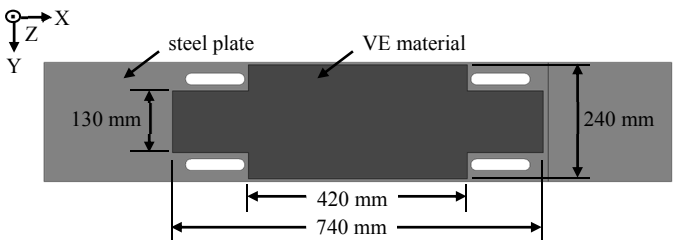

(c) Dimension of VE laminations (not to scale).

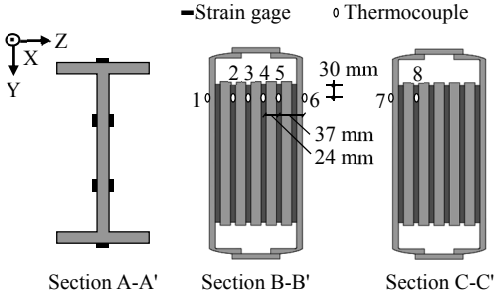

(d) Locations of strain gages and thermocouples.

Figure 2. Details of the VE damper test.

manufacturer are: shear modulus G = 3.92 N/cm2, fractional derivative order α = 0.558, at reference temperature θ_{ref} = 20.0°C, a_{ref} = 0.0056 and b_{ref} = 2.10, and p_1 = 14.06 and p_2 = 97.32.

2.2 Loading condition and measurements

The dynamic actuator was set to have sinusoidal deformation at 0.50 Hz (period T = 2.0 seconds) with peak value of ±5.0 mm. This harmonic deformation was continuously applied to the VE damper test assembly for 3.0 hours (5,400 cycles).

Figure 2d shows the locations of the strain gages and thermocouples used to measure the damper force F_d and temperature θ, respectively. There were 6 strain gages placed at section A-A' to measure the strain used to calculate F_d. Measurements of strains were done at 0.01-second interval for the entire loading duration. Thermocouples were placed at sections B-B' and C-C' to monitor the temperature inside the VE laminations (i.e., points 2~5 and 8) and the steel surface (i.e., points 1, 6 and 7). In addition, two thermocouples were used to measure the indoor ambient temperature. One was placed 8 cm from the VE damper surface (Air Near) and the other one 86 cm from the VE damper (Air Far). All the temperature measurements were done at 0.50-second interval during the loading duration and continued 12 hours after the loading. The initial temperatures were observed to be around 5.0°C.

As mentioned above, strain gage type transducers were used to monitor the actual deformations along the X-direction of the different components of the test assembly. The deformations were measured at 0.01-second interval for the entire loading duration.

3 EXPERIMENTAL RESULTS

3.1 Measured temperature

Figures 3a-3c show the time-history of the measured temperature θ at different locations inside the VE materials and outside on the steel. Temperatures were recorded during the application of the harmonic loading (i.e., for 10,800 seconds or 3 hours), and continued for another 12 hours after the loading. During the application of the loading, the heat was continuously generated, significantly increasing the damper temperature. Since the laminated VE materials have low thermal conductivity, the generated heat flows at a significantly lower rate in the laminations that in the steel parts. For this, heat is mostly accumulated within the laminations. In general, the VE laminations have higher recorded temperature than in the steel parts. From the initial temperature of around 5.00°C, the maximum recorded temperature inside the VE lamination (at point 3) is 51.27°C and on the steel part (at point 6) is 31.73°C after the 3 hours. Upon the termination of the harmonic loading, heat generation immediately stopped. The ambient and damper temperatures were continuously recorded and observed for 12 hours. About this time, the temperature returned to its initial condition values.

Figure 3d shows the measured ambient temperature at two locations. The thermocouple located 8.0 cm away from the steel surface of the VE damper (Air Near) detected a maximum increase of about 7.50°C in ambient temperature during the entire duration of measurement. From the initial recorded value of 7.04°C, the maximum recorded temperature in Air Near is 14.43°C. Similar to the measurements on the VE damper, the temperature at Air Near decreases after the application of the loading, indicating that the rise in temperature was due to the generated heat from the vibration and not from the environment. As for the thermocouple located 86.00 cm from the VE damper (Air Far), it detected a maximum increase of about 2.50°C in ambient temperature. From the initial recorded value of 5.69°C, the maximum recorded temperature in Air Far is 8.03°C.

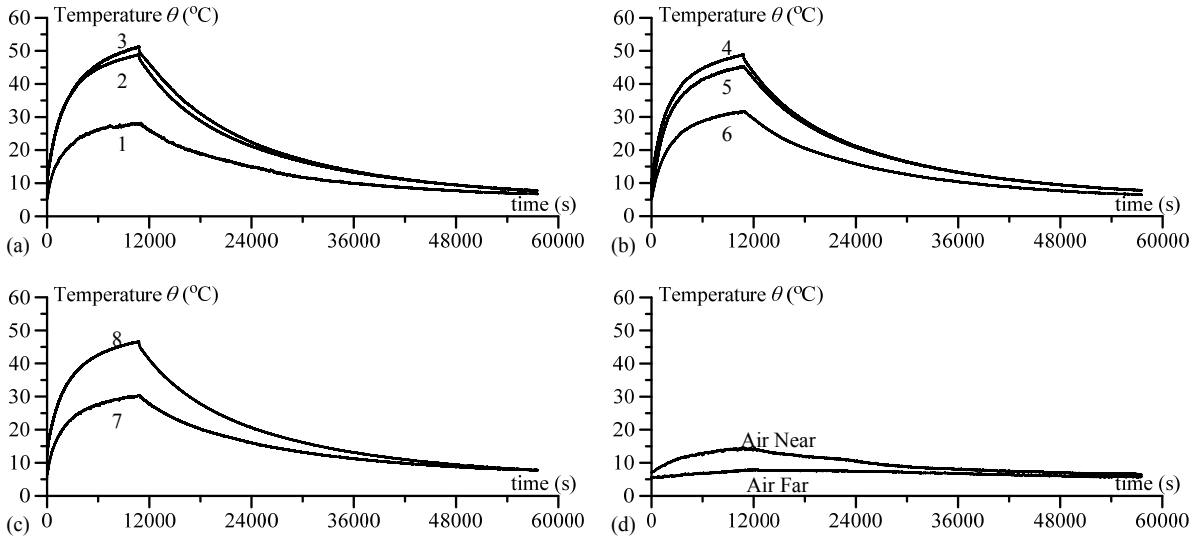

Figure 3. Time-history of measured temperature θ.

Moreover, the heat generation and heat transfer aspects in the beginning of the harmonic loading are investigated. Figure 4a shows the magnified temperature history of points 1, 2 and 3 from t = 0 s to 300 s. Immediately after the actuator was initiated, heat was generated and the temperature in the VE laminations (points 2 and 3) increased abruptly. As the generated heat within the VE laminations flowed to the steel parts, temperature in point 1 was starting to increase. However, due to the low thermal conductivity of VE materials, it took about 75 seconds for the steel part at point 1 to have a significant increase in

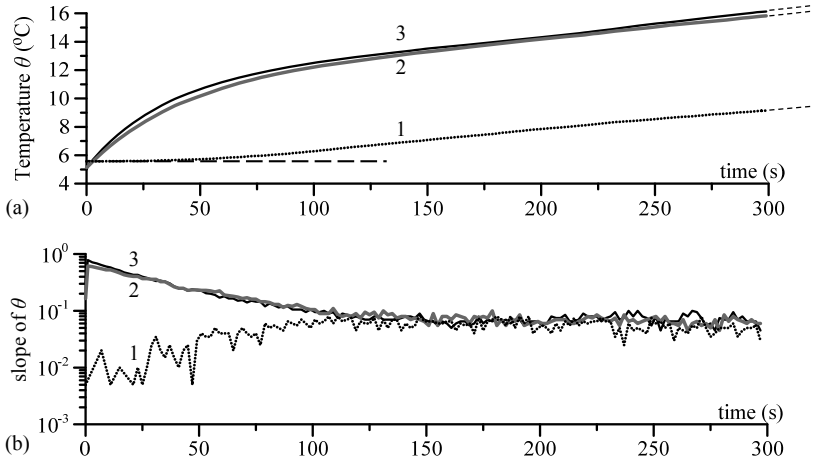

Figure 4. (a) Magnified plots of temperature θ at the beginning of the harmonic loading and (b) slope of temperature θ curves.

temperature. Heat was continuously generated and transferred as the experiment progressed. At about t = 100 seconds, the rates of temperature rise at points 1, 2 and 3 were almost the same.

Figure 4b shows the rate of temperature increase or slope of temperature time-history plots in Figure 4a. From t = 0 s to 100 s, rate of temperature increase of point 1 (steel part) was increasing while those in points 2 and 3 (VE laminations) were slowing down. This indicates that heat transfer aspect is gradually taking effect. After 100 seconds, all the three temperature measurements had almost the same rate of temperature increase or equal slope of about 0.01°C/second. Although sufficient amount of heat was transferred to the surrounding air, the temperature kept on increasing because, at this early stage of loading, the rate of heat generation was greater than the rate of heat transferred to the surrounding. As will be discussed in the succeeding sections, the VE laminations softens as the loading progressed, thus, the rate of heat generation decreases in the later stages of the long-duration test.

3.2 Deformations

Figure 5 shows time-histories of actuator deformation u_{act}, slider deformation u_{slider}, and damper deformation u_d at t = 0 s to 20 s and t = 10,000 s to 10,020 s. It was desired that the peak deformations of the actuator and the slider to be ±5.0 mm and ±10 mm, respectively. The amplification mechanism in the test rig (*see* Figure 2b) was to ideally amplify the actuator deformation u_{act} by a factor of 2.0 to produce the slider deformation u_{slider}. Damper deformation u_d was then expected to be almost equal to u_{slider} at any given instance. However, since the initial temperature was very low, the VE laminations were significantly stiff. It has been known that VE materials are temperature and frequency sensitive [2]. For this, the deformation initiated by the dynamic actuator was not effectively translated to damper deformation during the early loading cycles. Despite these, the peaks of u_{act} were close to the desired value of ±5.0 mm over the entire loading duration. As the damper temperature rose from dissipating kinetic energy, the VE laminations softens. It can then be observed that the deformation initiated by the actuator were effectively translated to the slider and the VE laminations.

Major deformation loss at the early stages of loading was between the u_{act} and u_{slider}. Figure 6 compares the peak deformations per cycle of test results. Here, the peak deformation per cycle is defined as the average of the positive and negative

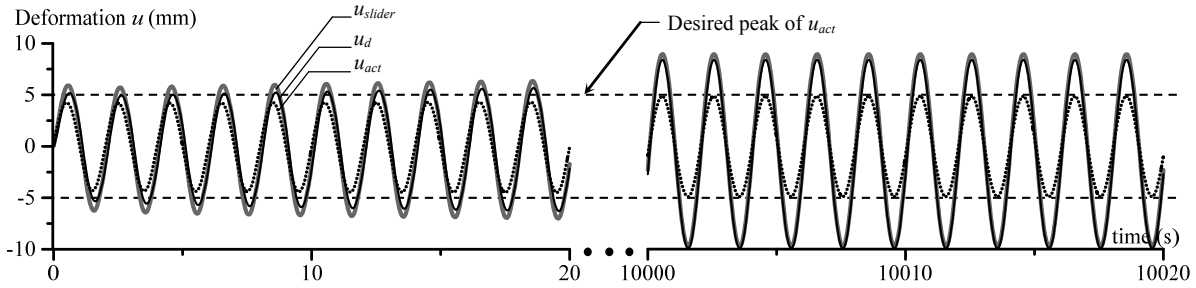

Figure 5. Recorded deformations of actuator u_{act}, slider u_{slider}, and damper u_d.

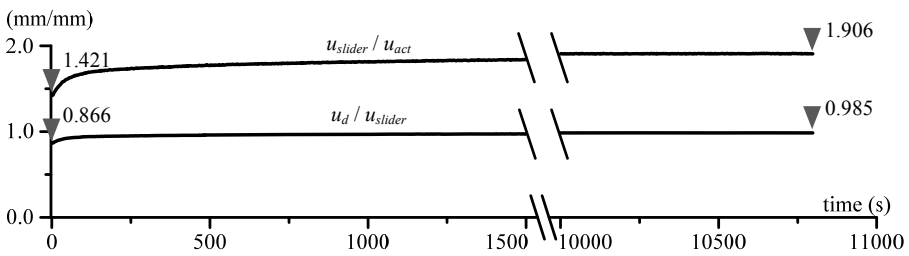

Figure 6. Comparison of recorded peak deformations.

peaks per cycle. At the first cycle, the ratio u_{slider}/u_{act} = 1.421 only which shows that the initiated deformation was not effectively amplified as desired. The amplification mechanism was subjected to unexpected relatively large deformation from the large damper force at the start since the VE laminations had high initial stiffness (discussed in the succeeding section). Eventually, amplification increases as the loading continuous and reached a maximum of 1.906 at the last cycle. For the ratio u_d/u_{slider}, the initial value was 0.866 which indicates that the steel brace along the length L (*see* Figure 2b) axially deformed by an amount equal to $0.134u_{slider}$. In spite of this, significant amount of the u_{slider} was translated to be u_d for most of the loading duration. At the end of the loading, the ratio u_d/u_{slider} reached 0.985.

3.3 Stiffness

The dynamic properties of the full-scale VE damper is determined by storage stiffness K'_d and loss stiffness K''_d. Figure 7a shows a typical hysteresis of steady-state damper force F_d and deformation u_d. From this hysteretic relationship, K'_d is defined as force at maximum deformation F'_d divided by the maximum deformation u_{d0}, and K''_d is defined as force at zero deformation F''_d divided by u_{d0}. In a similar manner, the storage modulus G' and loss modulus G'' can be defined from the hysteretic relationship of stress τ and strain γ as in Figure 7b. Also, loss factor η is determined by taking the ratio between G'' and G'.

As the storage stiffness K'_d represents the slope of the inclined ellipse (Figure 7a), its value can also be estimated by calculating the least-squares regression line of the recorded data per cycle, i.e.,

$$K'_d = \frac{n\Sigma\left(u_d^{(i)} \cdot F_d^{(i)}\right) - \Sigma u_d^{(i)} \Sigma F_d^{(i)}}{n\Sigma\left(u_d^{(i)}\right)^2 - \Sigma\left(F_d^{(i)}\right)^2} \tag{1}$$

where n = number of data per cycle.

Since the VE damper has relatively high initial stiffness and a possible machine-caused-error at the initiation of the dynamic actuator, it is imperative to define what constitutes cycle 1 for calculating the dynamic properties. Figure 7c shows the first 3 half waves of the F_d-u_d curve. Half wave 1 is from point o to point p, half wave 2 is from point p to point q, and half wave 3 is from point q to point r. This paper defines cycle 1 by neglecting half wave 1 and considers the combinations of half wave 2 and half wave 3 only. Not shown here, but it follows that cycle 2 is composed of half wave 4 and half wave 5.

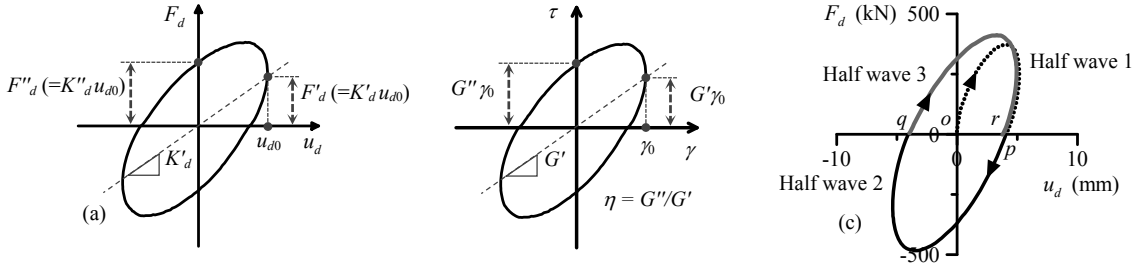

Figure 7. (a) Typical steady-state elliptical hysteresis, and (b) definition of cycle 1 of the harmonic loading test.

Figure 8a shows the time-history of K'_d following the Equation 1 and above definitions. The VE damper had a high K'_d value at the beginning of the loading since its initial temperature was very low. However, after only few cycles, its K'_d value abruptly dropped. From K'_d = 52.714 kN/mm at cycle 1, it dropped to 37.742 kN/mm at cycle 10. It continued dropping to 6.682 kN/mm at cycle 1500 and to 4.892 kN/mm at cycle 5400 (end of the loading). The average decrease rate of K'_d is 1.6636 kN/mm per cycle between cycles 1 and 10, 0.0208 kN/mm per cycle between cycles 10 and 1500, and 0.0005 kN/mm per cycle between cycles 1500 and 5400. This decreasing rate of change is attributed to the amount of heat generated per cycle and to heat transferred to the surrounding air.

Figure 8b shows the hysteresis loops at different cycles. As the experiment progressed, the damper temperature increases (Section 3.1), softening the VE material, and lowering the amount of energy dissipated. Cycles 1 and 10 have steep inclinations and fat loops, dissipating large amount of energy when the damper temperature is low. Cycles 100 and 1500 have small inclinations and slim loops, dissipating small amount of energy when the damper becomes warmer. With less energy dissipated per cycle, the corresponding amount of heat generated is also less. Adding in the aspect of heat transfer causes the damper temperature θ increase to becoming sluggish. As a result, rate of K'_d decrease becomes sluggish as well.

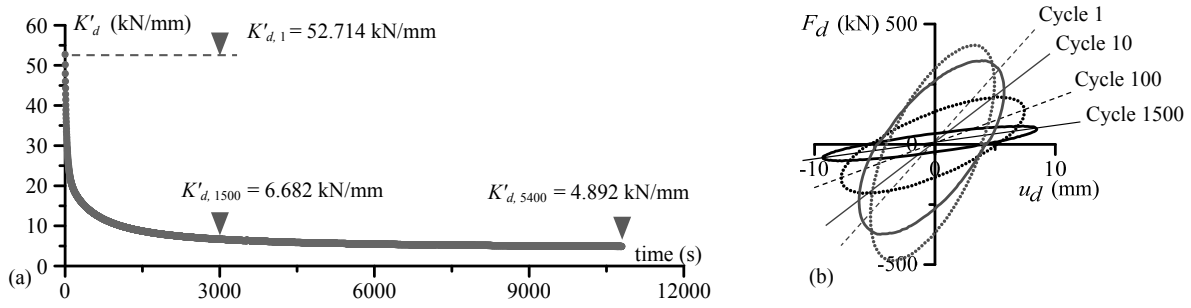

Figure 8. Test results: (a) time-history of K'_d, and (b) hysteresis at different cycles.

4 ANALYSIS USING THREE-DIMENSIONAL FINITE-ELEMENT METHOD

In 2006, Kasai *et al*. [7] proposed a method to analyze a simple two-layered VE damper subjected to long-duration loading. Their model combined static analysis and heat transfer analysis using three-dimensional finite elements, thus, referred as 3D-FEM model. The said model is adopted in the analysis of the full-scale multi-layered VE damper discussed in Chapters 2 and 3. This chapter presents an overview of the 3D-FEM model, followed by the modeling of the VE damper specimen. Results are then compared with the test.

4.1 Overview of the 3D-FEM model

The 3D-FEM simulates the temperature and frequency dependencies of the VE materials. The initial temperature of the VE damper is set. It follows that the storage modulus G'_j and loss factor η_j of each of the VE material element j for the known initial temperature are calculated as

$$G'_j = G\frac{1+a_jb_j\omega^{2\alpha}+(a_j+b_j)\omega^{\alpha}\cos(\alpha\pi/2)}{1+a_j^2\omega^{2\alpha}+2a_j\omega^{\alpha}\cos(\alpha\pi/2)} \quad \text{and} \quad \eta_j = \frac{(-a_j+b_j)\omega^{\alpha}\sin(\alpha\pi/2)}{1+a_jb_j\omega^{2\alpha}+(a_j+b_j)\omega^{\alpha}\cos(\alpha\pi/2)}. \tag{2a and 2b}$$

Here, ω = circular frequency (rad/s), α = fractional derivative order, and a_j and b_j are functions of the shift factor λ calculated as

$$a_j = a_{ref}\,\lambda_j^{\alpha}, \quad b_j = b_{ref}\,\lambda_j^{\alpha}, \quad \lambda_j = \exp\left[-p_1(\theta_j-\theta_{ref})/(p_2+\theta_j-\theta_{ref})\right]. \tag{3a ~3c}$$

where a_{ref} and b_{ref} are values at reference temperature θ_{ref}. It follows that the storage modulus for axial direction E'_j can be calculated as functions of G'_j and Poisson's ratio ν, i.e.,

$$E'_j = 2G'_j(1+\nu). \tag{4}$$

<u>*Static analysis*</u>. After setting the initial conditions, static analysis for each cycle can begin. Subject the damper to a maximum deformation of u_{d0} and reaction force F'_d is calculated. Multiplying the total strain energy of the viscoelastic elements by $2\pi\eta_j$ approximates the energy dissipated per cycle $W_{d,j}$, as in

$$W_{d,j} = \pi\eta_j V_j\left\{\sum_{k=1}^{3} E'_j\,\varepsilon_{kk,j}^2 + G'_j\left(\gamma_{12,j}^2+\gamma_{23,j}^2+\gamma_{31,j}^2\right)\right\} \tag{5}$$

where V_j = volume of element j, $\varepsilon_{mn,j}$ and $\gamma_{mn,j}$ = strains at the center of the element. The rate of heat generation per unit volume $\dot{q}_j$ for the corresponding cycle is then approximated by

$$\dot{q}_j = W_{d,j}/(V_j\,T). \tag{6}$$

The storage stiffness K'_d and loss stiffness K''_d for the corresponding cycle are estimated as

$$K'_d = F'_d/u_{d0} \quad \text{and} \quad K''_d = \left(\sum_j W_{d,j}\right)\Big/\left(\pi u_{d0}^2\right). \tag{7a and 7b}$$

<u>*Three-dimensional heat transfer analysis*</u>. After the approximation of the rate of heat generation per unit volume, heat transfer analysis is carried out. Damper is reset to zero deformation. Using the estimated rate of heat generation per volume $\dot{q}_j$ from Equation 6, 3D heat transfer analysis is carried out for T time corresponding to the current cycle. The new VE damper temperature serves as the initial condition for the next cycle.

Using the updated temperature of the VE laminations, the properties G'_j, η_j and E'_j are recalculated (Equations 2 and 3). The static analysis is carried out again, followed by the heat transfer analysis. These steps are repeated for the required number of cycles.

4.2 Implementation of the 3D-FEM model

4.2.1 Damper model for analysis

Figure 9 show the 3D model of the full-scale VE damper. The commercially available finite element software ABAQUS 2017 was used in the analysis with a FORTRAN subroutine made to model the material properties and to calculate the heat generation per simulated cycle. Coupled temperature-displacement solid elements were used. Figure 9a shows the interior assembly of the steel plates (PL01 to PL03) and VE laminations, and Figure 9b shows the whole damper assembly. Steel plates PL01 and PL03 are connected to the steel part subjected to deformation, while PL02 are connected to the fixed-end steel part.

Since the *X*-*Y* midplane and *X*-*Z* midplane are planes of symmetry, only a quarter section of the whole damper is used in the analysis as in Figure 9c. The VE laminations are designated as VE01 to VE03 for convenience in the succeeding sections, with the VE01 being the outermost layer and VE03 being the innermost layer. The thickness of each VE laminations was divided in 6 elements while mesh size in the *X*- and *Y*-directions is close to 10 mm.

4.2.2 Damper properties

In addition to the damper properties given in Section 2.2, the following parameters are used for the 3D heat transfer analysis: for steel, κ_{steel} = 43.128 N/s/°C, s_{steel} = 46.63 x 10^3 N·cm/kg/°C and ρ_{steel} = 7.80 x 10^{-3} kg/cm^3, and for VE laminations, κ_{VE} = 0.188 N/s/°C, s_{VE} = 19.40 x 10^4 N·cm/kg/°C and ρ_{VE} = 1.00 x 10^{-3} kg/cm^3, and for VE laminations.

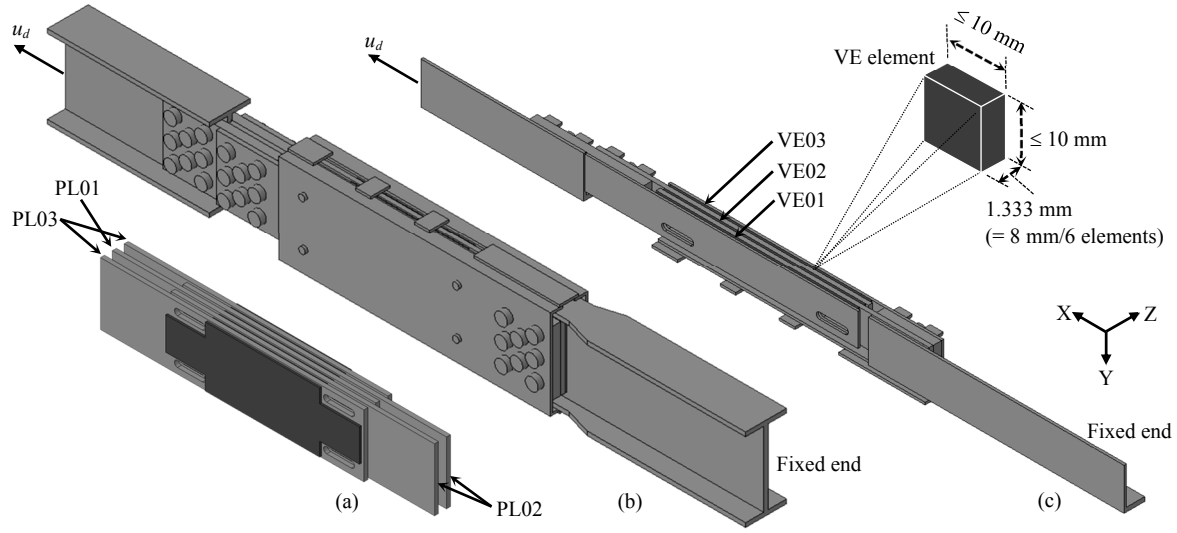

Figure 9. 3D-FEM model of the full-scale VE damper: (a) interior assembly of steel plates and VE laminations, (b) whole damper assembly, and (c) quarter section considered for the analysis.

Unlike κ, s and ρ which are thermophysical properties of a material, heat transfer coefficient α_c is a system property [8]. It depends on several flow parameters such as relative velocity between material surface and surrounding air, and their difference in temperature. Gopalakrishna and Lai [9] and De Cazenove *et al*. [10] pointed out that approximation of heat transfer coefficient is difficult. For this, a trial-and-error approach was adopted in implementing 3D-FEM analysis. Several values of α_c was tried to match well with the recorded and the adopted the following values: All parts other than those in the interior assembly have α_c = 7.50 N/s/m/°C, PL01 has α_c = 2.00 N/s/m/°C, PL02 has α_c = 1.00 N/s/m/°C, and PL03 has α_c = 3.00 N/s/m/°C. A small α_c value was assigned to PL02 since it was not a moving plate. For the air-exposed surface of VE laminations, the α_c assigned to its closest laminating steel is adopted. Take VE01 as an example: Since it is attached to PL01 and PL02, then 50% of its air-exposed surface had α_c = 2.00 N/sC and the remaining 50% of the air-exposed surface had α_c = 1.00 N/s/m/°C.

4.2.3 Loading conditions

To simulate the test setup, the recorded ambient temperature Air Near θ_{Near} (Figure 3d) and damper deformation u_d (Figure 5) were used as input data. The recorded θ_{Near} at the beginning of one cycle is taken as the corresponding ambient temperature for the simulated cycle. The average of the recorded positive and negative peak deformations for one cycle is taken as the corresponding damper deformation for the simulated cycle.

4.3 Results of the 3D-FEM analysis

Figure 10 shows the predicted (black dots) and the measured (gray lines) temperatures θ. Only the time-history during the loading is reported in this paper. Figures 10a and 10b are those of Section B-B' while Figure 10c are those of Section C-C'. Predicted temperature in point 1 (steel surface) has the largest discrepancy among all others. Despite these discrepancies, generally, the predicted θ fairly agrees with the test.

The above comparisons of temperature, however, represent only a very minute part of the VE damper. The sum total behavior to be reckoned with is the dynamic property of the VE damper. Figure 11 shows the K'_d time-histories from the analysis (black line) and the test (gray line). The 3D-FEM prediction matches well with the recorded data.

Moreover, Figure 12 shows the 3D-FEM temperature distributions at t = 3.0 hours. Figure 12a depicts the quarter section temperature scaled from 0°C to 60°C. Due to the VE laminations' low thermal conductivity, heat accumulates in the innermost parts of the VE damper. The maximum predicted θ is 54.35°C at VE01. The whole damper temperature is depicted in Figure 12b. The exterior surface temperature reached a maximum of 37.30°C which is relatively lower than the interior assembly temperature.

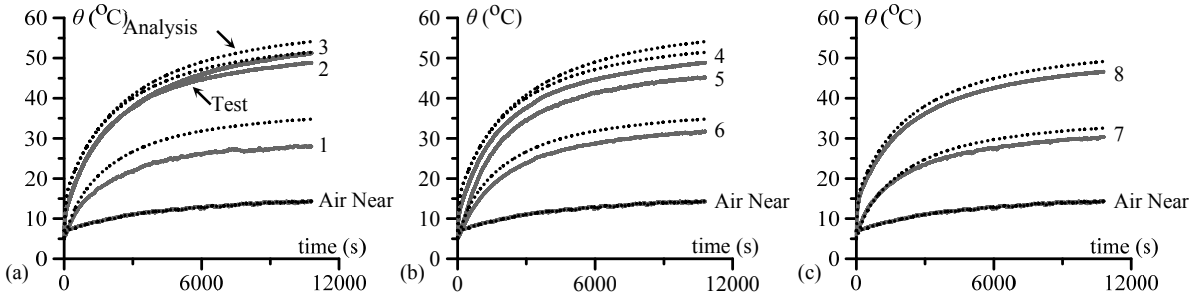

Figure 10. Temperature θ: Analysis vs. experiment.

Figure 12c shows the VE laminations temperature distributions with a contour scaling of 20°C to 60°C. The predicted θ for VE01 range from 29.41°C to 54.35°C, for VE02 range from 28.83°C to 52.60°C, and for VE03 range from 23.12°C to 48.01°C. All of the maximum θ are found in the mid-portions of the VE laminations, and all of the minimum θ are found at the ends of the VE laminations.

Figure 12d shows the temperature distributions at sections B-B' and C-C' with a contour scaling of 20°C to 60°C. The predicted θ for section B-B' is 54.35°C and for section C-C' is 51.87°C. As expected, section B-B' has higher distributions than section C-C' since it is situated in the middle of the VE damper. Due to the high thermal conductivity of steel, the temperature on the exterior steel parts is distributed almost uniformly.

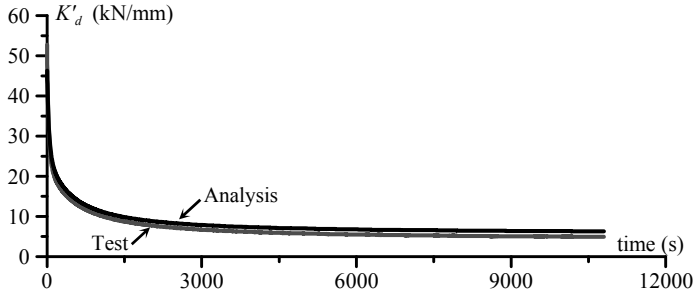

Figure 11. Storage stiffness K'_d: Analysis vs. experiment.

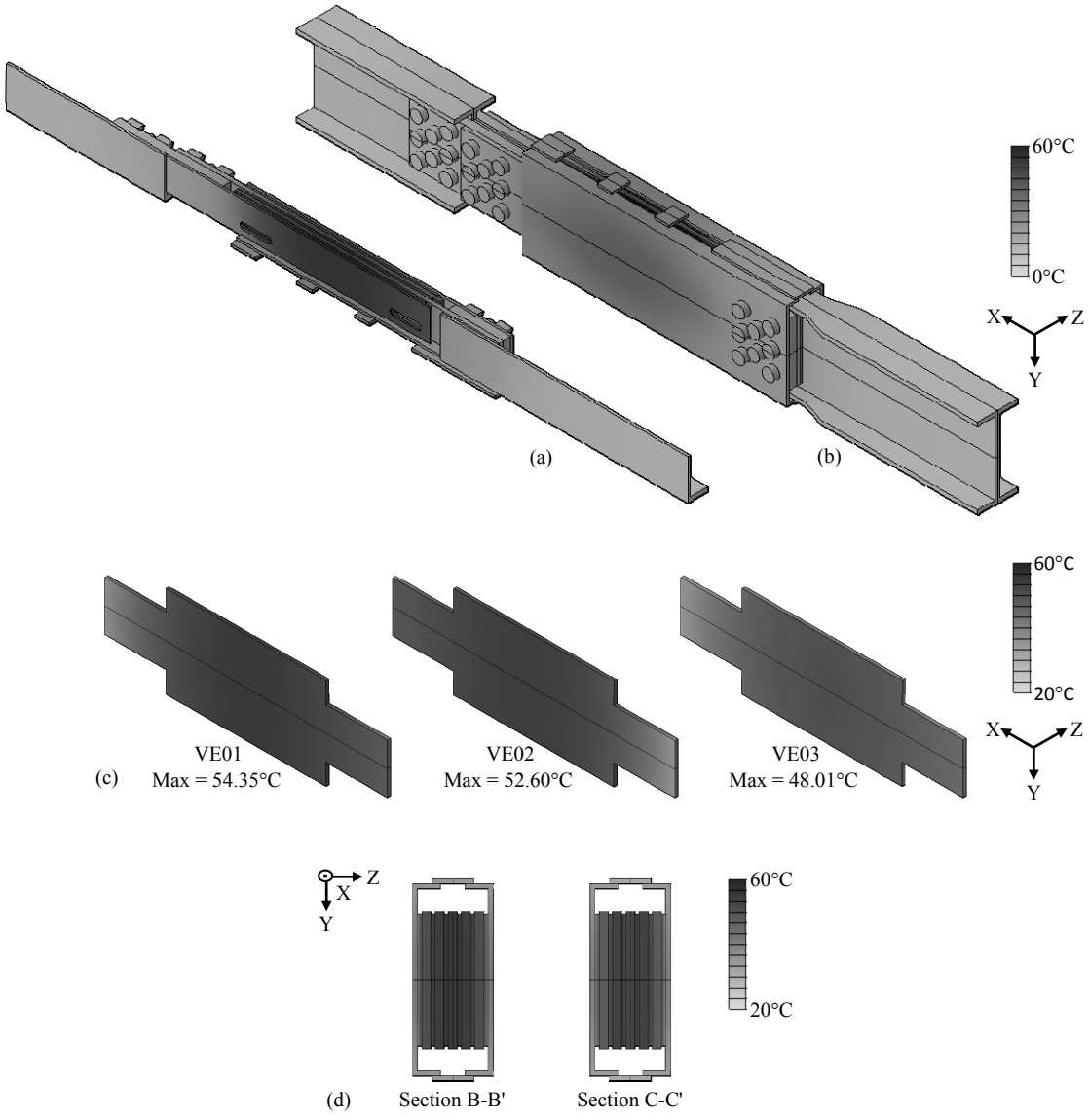

Figure 12. Temperature distributions at t = 3 hours (10,800 seconds). (a) and (b) quarter section and whole damper assembly, respectively, (c) VE laminations, and (d) cross-sections B-B' and C-C'.

5 CONCLUSIONS

This paper experimentally and analytically showed the behavior of a full-scale multi-layered viscoelastic damper subjected to long-duration harmonic loading at a low ambient temperature of about 5°C. With this very low initial temperature, the damper had a very high initial stiffness. As such, the damper absorbed relatively large amount of kinetic energy at the early loading stages resulting to rapid increase of temperature at the start. Eventually, the VE laminations softened as the loading continued, and the temperature increased gradually.

For the entire duration of the measurement, the innermost VE laminations had higher temperature than those innermost steel plates. Since the VE laminations have low thermal conductivity, the generated heat accumulates inside the VE laminations. It required a significant amount of time before it was transferred to the steel parts and dispersed to the surrounding air. Experimental investigation on the beginning of the loading showed that it took about 100 seconds (50 cycles) before the temperature on the exterior steel surfaces increased significantly.

It was also shown in this paper that the 3D-FEM model proposed by Kasai *et al*. [7] can be adopted to predict the dynamic behavior of a more complex VE damper configuration. The predicted behavior of full-scale VE damper specimen agreed fairly with the recorded test data. However, the analyses were still based trial-and-error approach because the heat transfer coefficient remains difficult to estimate, as also adopted by other researchers.

Despite the complex geometrical configuration of a full-scale VE damper, its behavior under long-duration loading at low ambient temperature can be predicted with good accuracy.

ACKNOWLEDGEMENTS

This work was supported by JST Program on Open Innovation Platform with Enterprises, Research Institute and Academia (OPERA). We are also grateful to Assoc. Prof. Kazuhiro Matsuda (Meijo Univeristy, Japan), and to Mr. Hitoshi Takimoto and Mr. Fumiya Ueno (both graduate students of Tokyo Institute of Technology, Japan) for their invaluable assistance in the preparation and conduct of the experiment.

REFERENCES

[1] Nielsen EJ, Lai ML, Soong TT, Kelly JM. Viscoelastic damper overview for seismic and wind applications, Proceedings: SPIE 2720, Smart Structures and Materials 1996: Passive Damping and Isolation.

[2] Nashif AD, Jones DIG, Henderson JP. *Vibration Damping*. England: John Wiley & Sons Ltd; 1985.

[3] Mahmoodi P, Robertson LE, Yontar M, Moy C, Feld L. Performance of Viscoelastic Structural Dampers in World Trade Centre Towers, Dynamics of Structures Congress 1987, Orlando, Florida, USA.

[4] Mahmoodi P, Keel CJ. Performance of Viscoelastic Structural Damper for Columbia Centre Building. In: *Building Motion in Wind* (Eds N Isyumov and T Tschanz), ASCE, 1987, New York, USA. pp 83-106.

[5] Sato D, Kasai K, Sakaibara N. Experiment of Full-Scale Viscoelastic Damper and Analysis due Change in Dynamic Characteristics under Long-Period Ground Motion. Summaries of Technical Paper of Annual Meeting, Architectural Institute of Japan (AIJ). September 2014:1009-1110 (In Japanese).

[6] Montgomery M and Christopoulos C. Experimental Validation of Viscoelastic Coupling Dampers for Enhanced Dynamic Performance of High-Rise Buildings. Journal of Structural Engineering, ASCE. 2015;141:04014145(11).

[7] Kasai K, Sato D, Huang Y. Analytical Methods for Viscoelastic Damper Considering Heat Generation, Conduction and Transfer under Long Duration Cyclic Load. *Journal of Structural and Construction Engineering* (Transactions of AIJ). 2006; 599:61-69 (In Japanese).

[8] Zhang J, Delichatsios MA. Determination of the Convective Heat Transfer Coefficients in Three-Dimensional Inverse Heat Conduction Problems. Fire Safety Journal. 2009;44:681-690.

[9] Gopalakrishna HS, Lai ML. Finite Element Heat Transfer Analysis of Viscoelastic Damper for Wind Applications. *Journal of Wind Engineering and Industrial Aerodynamics*. 1998;77&78:283-295.

[10] De Cazenove J, Rade DA, De Lima AMG, Araujo CA. A Numerical and Experimental Investigation on Self-Heating Effects in Viscoelastic Dampers. Mechanical Systems and Signal Processing. 2012;27:433-445.